ELSEVIER

Earth and Planetary Science Letters 134 (1995) 527–544

EPSL

The effect of rift shoulder erosion on stratal patterns at passive margins: Implications for sequence stratigraphy

R.T. van Balen *, P.A. van der Beek, S.A.P.L. Cloetingh

Institute of Earth Sciences, Vrije Universiteit, De Boelelaan 1085, 1081 HV Amsterdam, The Netherlands

Received 10 April 1995; accepted 25 July 1995

Abstract

Numerical modelling indicates that the erosion of uplifted rift flanks at passive margins has a profound effect on offshore stratigraphic patterns. Flexural uplift, due to isostatic rebound in response to erosion, extends far into the basin and causes uplift of the shelf. As a result, the contemporaneously deposited sedimentary wedge displays a characteristic offlap pattern. When the rift shoulder is largely eroded, onlap-promoting mechanisms related to cooling of the lithosphere enable sediments to onlap onto the basin margin. The initial offlapping and subsequent onlapping strata form one complete second-order depositional sequence comprising a shelf-margin-, transgressive-and highstand-systems tract. The modelling inferences are in broad agreement with stratal patterns and basin geometries observed on the U.S. east coast, the southeastern Brazilian and southeastern Australian passive margins and the Transantarctic Mountains–Ross Sea Shelf system. The initial offlaps caused by erosion of rift shoulders have important implications for the deriviation of eustatic signals from coastal onlap patterns.

1. Introduction

Uplifted flanks are a common feature of young rifts. The rift flank morphology is typically asymmetric and consists of a steep slope facing the rifted basin and a gentle slope extending in a landward direction away from the 2–3 km high flank summit. Modern examples include the Gulf of Suez, the northern Red Sea, the Transantarctic Mountains and the East African Rift systems [1–3]. Apatite fission track studies have revealed that large amounts (3–4 km) of basement rocks have been eroded from the present-day coastal plains of the South African [4–6], South American [7], U.S. east coast [8,9] and southeastern Australian [10,11] passive margins, providing evidence for uplift and erosion of rift flanks at these margins [3]. At present, the passive margins of South America, South Africa and southeastern Australia are associated with an erosional escarpment located about 100 km landward of the shoreline.

Continuous coastal onlap is commonly regarded to be a general feature of rifted basins and passive margins and is intrinsically caused by tectonic subsidence. Punctuations in the long-term onlap pattern are explained by eustatic sea-level changes and tectonically induced on-and offlap events [12–14]. Based on evidence from the Gippsland Basin and the U.S. east coast passive margin, Watts et al. [15] showed that long-term, large-scale stratigraphic onlap onto basin margins is consistent with the results of an elastic flexure model in response to sedimentary and lithospheric loads. They concluded that an

* E-mail balr@geo.vu.nl; fax +31-20-6462457

SSDI 0012-821X(95)00029-1

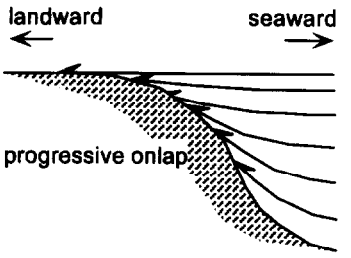

Fig. 1. Long-term continuous onlap in an elastic model of basin evolution (after [15]). Increasing thermal and sedimentary loads, as well as the thermally controlled increase in flexural rigidity, cause a widening of the basin with time and, therefore, stratigraphic onlap.

increase in flexural rigidity induced by cooling and the increase in loads with time, due to the weight of the sediments and contraction of the lithosphere, can explain the widening of a passive margin basin and associated continuous coastal onlap patterns (see Fig. 1). White and McKenzie [16] invoked differential stretching of crust and mantle to explain post-rift stratigraphic onlap at basin margins. In this model, the mantle part of the lithosphere is extended by the same total amount as the crustal part, but spread over a wider area. This results in post-rift thermal subsidence occurring at the flanks of the basin and, as a consequence, stratigraphic onlap. However, large-scale stratal patterns of various passive margins do not exhibit continuous coastal onlap, as demonstrated by, for example, Beaumont et al. [17], Galloway [14] and Watts [18].

The results of Watts et al. [15] were largely influenced by simplified assumptions regarding the distribution of basin fill—in their model the basin is always filled up to sea level. The observed progradational nature of many basin fills modifies the flexural deformation of the basin. Prograding sedimentary wedges have the highest sedimentation rates on the slope. Flexure due to the concentrated sediment loading at the slope results in enhanced subsidence at the slope and uplift in a landward direction. The uplift is located at the margin or the shelf, depending on the width of the prograding wedge and the flexural rigidity of the underlying lithosphere. If uplift takes place at the landward edge of the sedimentary wedge, a coastal offlap pattern will be formed [14,18] (Fig. 2). In their analyses, Watts et al. [15] also excluded the effect of rift shoulder uplifts. The steep onlap surface induced by an uplifted rift shoulder inhibits long-term large-scale stratigraphic onlap. Furthermore, erosion of a rift shoulder induces flexural uplift potentially extending far into the offshore basin, causing uplift of the shelf area and leading to stratigraphic offlap. As will be shown, numerical modelling of the effect of erosion of rift shoulders on offshore stratigraphy demonstrates that up to 20 km of offlap can be produced by this mechanism. When the rift shoulder is largely eroded, onlap-promoting mechanisms (related to cooling of the lithosphere

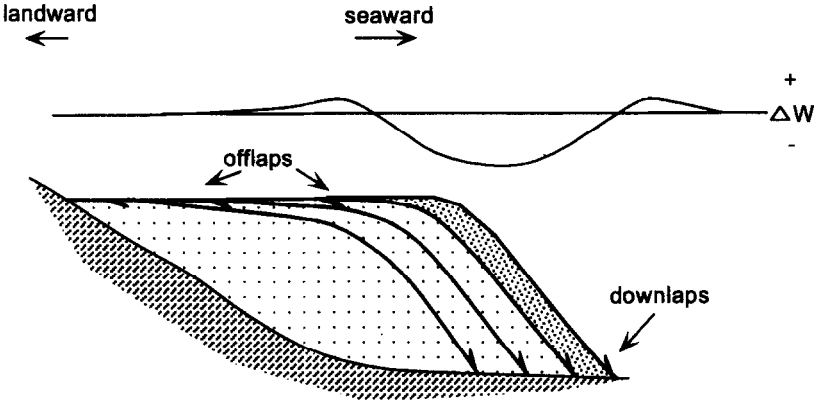

Fig. 2. A prograding sedimentary wedge causes a continuous basinward shift of the instantaneous sedimentary load. The flexural response to the load causes uplift in a landward position, leading to erosional truncation. Due to the basinward shift of the load, the bulge and shoreline also migrate basinward. Δw = flexural uplift (+) and subsidence (−) pattern due to progradation.

and loading by sediments) enable sediments to onlap onto the basin margin. Together, the initial offlapping and subsequent onlapping strata form one complete second-order depositional sequence.

The effect of rift shoulder uplift and erosion on offshore stratigraphy has not been investigated thoroughly yet. Only increases in offshore sedimentation rates have been attributed to an acceleration of flank erosion [4,5,19] or the breakthrough of the marginal upwarp by major interior river systems (e.g., the Orange and Zambezi Rivers in southern Africa) [4,20]. Our approach integrates a model for basin evolution with modelling of rift shoulder erosion and offshore sedimentation in the nearby extensional basin, thus treating the rift shoulder and extensional basin as one coupled system.

Below, we discuss examples of large-scale stratal patterns and former rift shoulder uplifts on the U.S. east coast, the southeastern Brazilian and southeastern Australian margins, and the Transantarctic Mountains–Ross Sea Shelf system. We subsequently demonstrate that part of the large-scale stratal pattern can be explained by flexural rebound in response to rift shoulder erosion.

2. Examples of passive margins

2.1. U.S. east coast margin

The passive margin of the U.S. east coast originates from Middle Triassic to Middle Jurassic rifting. As shown in Fig. 3a, the margin displays a characteristic morphology with, passing landward, a deep (13 km) elongate basin and a shallow (500 m), wide (200 km) coastal plain bordered by a 200 m piedmont and the Appalachian mountain range [9,22,23]. Halfgrabens filled with Triassic and Early Jurassic sediments are also located onshore, in the coastal plain area (Fig. 3a). The offshore basin fill consists of Triassic clastics, Jurassic evaporite, shale, chalk and platform margin carbonates and a mainly deltaic clastic succession ranging from Cretaceous to Recent in age [23]. The Jurassic sequences are largely aggradational and show offlap. The landward lap-out position extends about 20 km from the hinge zone (Fig. 3a). Cretaceous sediments demonstrate considerable coastal onlap and cover the coastal plain area. Paleogene chalks are deposited over a large part of the shelf. The Miocene to Recent clastic sediments are grouped in a number of depositional sequences, displaying an overall offlap pattern [24]. This pattern was interpreted by Watts [18] to be the result of coastal flexural uplift due to basinward sedimentary loading. This is consistent with a petrographic correlation of river terraces and coastal plain and basinal deposits, showing that the coastal plain area has continuously tilted basinward since the Early Miocene [22].

Apatite and zircon fission track data from the Newark Basin (an Early Mesozoic halfgraben located close the coastal plain) show evidence for a hydrological system perturbing the temperature field, which requires a paleorelief of 1–1.5 km located about 250 km landward of the hinge zone [9]. Furthermore, the apatite fission track ages demonstrate that flank erosion ended in the Late Jurassic ($\sim$ 140 Ma), which is supported by the onlap of Lower Cretaceous (124–118 Ma) sediments onto the present-day coastal plain. The estimated total amount of basement erosion is about 3 km in this area. The smooth warped surface of the syn-post rift boundary below the coastal plain and the absence of shallow-water syn-rift sediments in the halfgrabens is indicative of substantial (2–3 km) subaerial erosion (i.e., erosion of tilted fault blocks and part of the sedimentary fill in the grabens) [21]. These findings accord with evidence from a regional apatite fission track study in New York State [8], which points to completion of basement erosion in Early Cretaceous times, with 2–3 km of erosion in the western part of the state and 3–4 km of erosion in the northern part. To conclude, sufficient evidence exists for a former rift shoulder uplift on the U.S. east coast that was located at the position of the present-day coastal plain (Fig. 3a). This uplifted rift flank was mainly eroded during the Jurassic. Possible remnants of this shoulder can be found about 200 km landward of the shoreline (Blue Ridge and Catskill Hills). During erosion of the rift shoulder, a relative sea level fall occurred in the offshore basin, as is evident from the Jurassic stratigraphic offlap pattern. The position of landward lap-out occurs about 20 km basinward of the hinge zone. Present-day onshore uplift and offshore subsidence can be explained by erosional unloading (minor compared to rift shoulder erosion) at

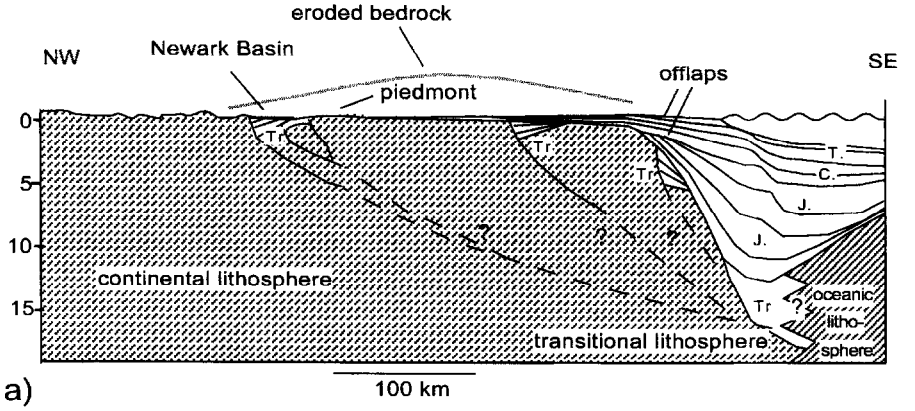
eroded bedrock
NW
Newark Basin
piedmont
offlaps
SE
0
5
10
15
Tr
T.
C.
J.
continental lithosphere
oceanic litho-sphere
transitional lithosphere ?
100 km

a)

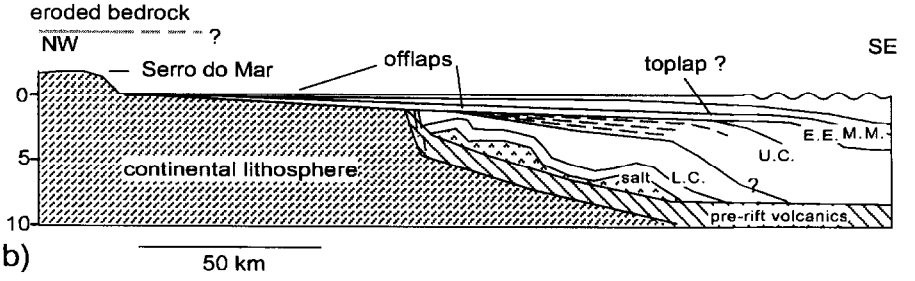
eroded bedrock
NW
?
Serro do Mar
offlaps
toplap ?
SE
0
5
10
E.E.
M.M.
U.C.
continental lithosphere
salt
L.C.
?
pre-rift volcanics
50 km

b)

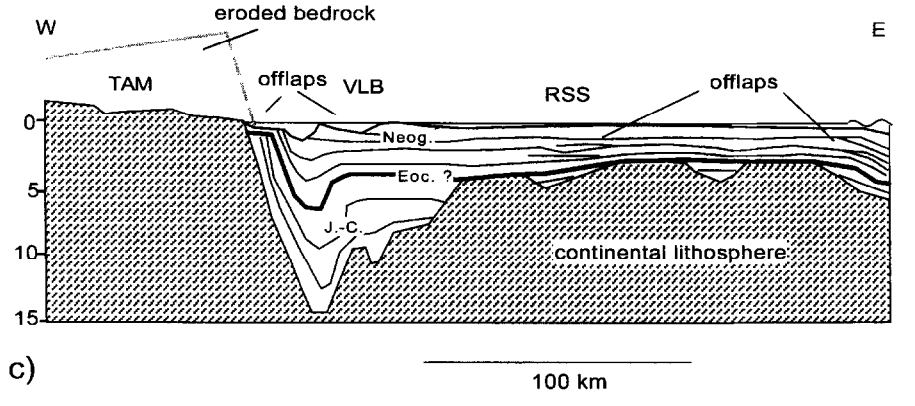
W
eroded bedrock
E
TAM
offlaps
VLB
RSS
offlaps
0
5
10
15
Neog.
Eoc. ?
J.-C.
continental lithosphere
100 km

c)

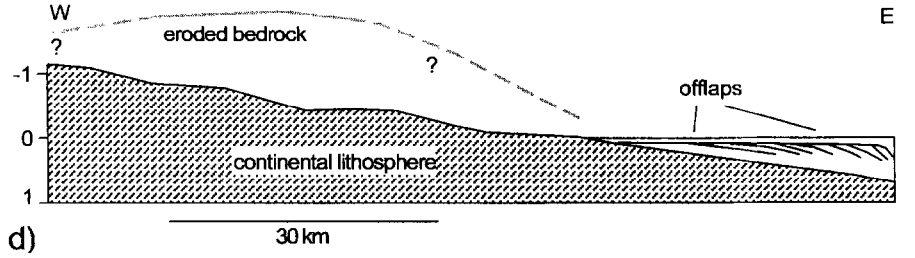
W
E
?
eroded bedrock
?
-1
0
1
offlaps
continental lithosphere
30 km

d)

a 200 m high escarpment and onshore loading due to deltaic progradation [18,22].

2.2. South Brazilian margin

The passive margin of southern Brazil originates from Early Cretaceous rifting (~ 140 Ma). At present, its physiography consists of a series of offshore coast-parallel basins, an 80 km wide coastal plain, and an inland elevated region (Fig. 3b). The basin fill consists of syn-rift volcanics and clastics (140–120 Ma) overlain by a series of evaporites and carbonates (mainly with Middle to Upper Cretaceous ages) and Middle to Late Tertiary clastics [7,19,25]. The Cretaceous post-rift sediments exhibit an initial stratigraphic offlap pattern succeeded by a toplap phase (Fig. 3b). The Eocene–Lower Miocene (52–16 Ma) clastics show considerable onlap onto the basement of the margin, covering the coastal plain area for the first time. The Middle to Late Tertiary (< 16 Ma) clastics demonstrate, again, offlap patterns [19,25]. Apatite fission track ages of onshore sedimentary and basement rocks indicate that about 3 km of overburden has been eroded in the coastal plain area, decreasing to 1 km more landward [7]; this points to a former rift flank uplift (Fig. 3b).

The large-scale Eocene–Lower Miocene stratigraphic onlap (80 km landward migration of the shoreline) demonstrates that the initial rift shoulder must have been almost completely eroded before the Eocene. The off-and toplap stratigraphic patterns of the Cretaceous post-rift sediments show that during the rift shoulder erosion a relative sea level fall occurred. The offlapping Miocene–Recent clastic sequences could be the result of flexural response to a combination of erosional escarpment retreat (now located 200 km landward from the position of the former rift flank uplift) and basinward deltaic progradation.

2.3. The Transantarctic Mountains and Ross Sea Shelf, Antarctica

The Transantarctic Mountains (TAM), a mountain range stretching from the Pacific side of Antarctica to the Atlantic Ocean, can be explained as a rift margin uplift resulting from extension in the west Antarctic rift system [26]. On the Pacific side of Antarctia, the TAM is bordered by the Ross Sea Shelf (RSS), a large basin system comprising three main sub-basins. The RSS system orginated from two extension phases, a widespread Mesozoic and a localized Early Cenozoic–Recent phase. The latter caused the present high elevation of the TAM [27]. The RSS contains several basins striking parallel to the TAM. The Victoria Land Basin (VLB), bordering the TAM, is the deepest. This contains 14 km of sediments, comprising about 10 km of Late Cretaceous–Eocene and about 4 km of Oligocene–Recent deposits [26,28,29]; the former are separated from the latter by an angular unconformity resulting from tectonic movements during the youngest extension phase (Fig. 3c). As a result of ongoing tectonism, the sediments close to the TAM in the VLB have been strongly deformed and uplifted and display an almost continuous coastal offlap pattern [27–29]. Offlapping stratal patterns eastward of the VLB are probably caused by erosional truncation due to glacial activity since the Oligocene [29], although tectonic influences cannot be excluded. Apatite fission track data and the present-day elevation of marker surfaces demonstrate that the TAM were uplifted 6 km since

Fig. 3. (a) Large-scale cross section through the U.S. east coast passive margin off New Jersey (after [21–23]). The grey line indicates the amount of eroded bedrock (based on [8,9,21]). The offshore stratigraphy displays offlapping Jurassic sequences, which can be explained by the flexural response to erosion of the marginal uplift. *Tr.* = Triassic; *J.* = Jurassic; *C.* = Cretaceous; *T.* = Tertiary. (b) Cross section through the south Brazilian margin (after [7,19,25]). The off-and toplapping stratigraphy of the Cretaceous sediments can be explained in terms of erosion of the marginal uplift. *L.C.* = Lower Cretaceous; *U.C.* = Upper Cretaceous; *E.E.* = Early Eocene; *M.M.* = Middle Miocene. (c) Cross section through the Transantarctic Mountains (*TAM*)–Ross Sea Shelf (*RSS*) system (after [26–29]). The Victoria Land Basin (*VLB*) displays a continuous offlapping steeply inclined stratigraphy, probably caused by ongoing tectonic uplift of the Transantarctic Mountain system. The tectonic uplift could be greatly enhanced by the flexural response to erosional unloading at the rift shoulder. *J.* = Jurassic; *C.* = Cretaceous; *Eoc.* = Eocene; *Neog.* = Neogene. (d) Generalized cross section through the southeastern Australian passive margin (after [10,11,30]). The offshore stratigraphy demonstrates continuous offlap which can be explained by regional eastward tilting due to erosional rebound at the rift shoulder.

the Early Eocene (55 Ma), 4.5–5 km of which have been eroded [26]. Modelling of rift shoulder uplift and erosion by Van der Beek et al. [3] demonstrated than an asymmetric extension model (subcrustal extension below the TAM) combined with flexural uplift best fits the observed data. Lateral heatflow from the nearby extended RSS may also contribute to thermal uplift [6].

Abundant normal faults cutting the entire stratigraphic section and active magmatism indicate that this margin is still extending. Therefore, the offlapping stratigraphy is interpreted as the result of extensional tectonics [27,28], although Vail et al. argue for eustasy-driven mechanisms [29]. Ongoing extensional tectonism would probably result in continuing subsidence in the VLB, whereas uplift is observed on its western rim. Therefore, we propose that flexural uplift as a response to erosion of the uplifted flank provides a more viable mechanism for explaining the observed offlap patterns in the VLB. The strongly deformed sediments and the observed offlaps in the stratigraphy serve as an additional indication of continuous Tertiary uplift and erosion of the TAM.

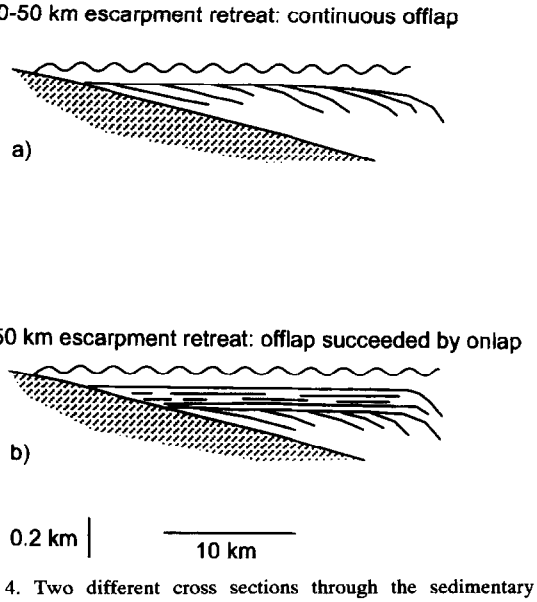

Fig. 4. Two different cross sections through the sedimentary wedge of southeastern Australia. (a) The generally occurring continuous offlap stratal pattern, related to a 10–50 km retreat of the marginal uplift. (b) The stratal patterns offshore Sydney. Only in this area is a major unconformity separating offlapping from overlying onlapping strata found. This location coincides with an area where the escarpment has retreated ~50 km more in a landward direction than elsewhere (after seismic data from [30]). See text for further discussion.

2.4. The southeastern Australian passive margin

The passive margin of southeastern Australia borders the Tasman Sea and originated from Late Cretaceous or Early Tertiary breakup (80–60 Ma). The rifting caused opening of the central Tasman Sea and uplift of the margin [10,11,30,31]. The passive margin fill consists of a very thin (~ 500 m) and narrow (~ 30 km) sedimentary wedge containing Tertiary to Recent clastic sediments [30]. The sediments demonstrate an almost continuous offlap pattern (Fig. 3d). Offshore Sydney, however, seismic data show a major unconformity of unknown age that separates underlying offlapping from overlying onlapping strata (Fig. 4). Along this part of the margin the escarpment has retreated ~ 50 km more than in neighbouring areas, indicating a close relationship between the amount of retreat of the escarpment and offshore stratal patterns.

Syn-rift uplift of the margin and subsequent erosion is evident from fission track [10,11] and geological and morphological data [31]. The long life span of the rift shoulder indicates a permanent uplift mechanism. Forward modelling of uplift and erosion by Van der Beek et al. [32] shows that a flexural mechanism cannot explain all the observed uplift. Van der Beek et al. observed that the amount of erosion could only be fitted by a model assuming a relatively young (20 Ma) thermal uplift event. However, there is no evidence for such an event in the offshore stratigraphy.

At present, the margin is accompanied by an erosional escarpment located several tens to 100 km inland and attaining heights of up to 1 km [33]. The amount of erosion and uplift in the coastal area indicated by the fission track data is between 1.5 and 4 km. The offlapping strata indicate a continuous regional eastward tilting of the shelf area. The same eastward tilting was inferred onshore by Ollier [33] on the basis of paleoflow directions of rivers, seaward of the present-day escarpment.

2.5. Summary

The examples discussed above demonstrate that large amounts of erosion have occurred at the pre-

sent-day coastal plains of passive margins and the TAM–RSS system, indicating the occurrence of former uplifted rift shoulders. Offshore off-and toplapping stratal patterns point to a regional relative sea level fall occurring in the offshore basins during erosion of the rift shoulder. These stratal patterns are traditionally interpreted in terms of eustatic sea level changes or are ascribed to tectonic causes [12–14]. However, the synchroneity of offshore stratigraphic offlap with rift shoulder erosion and, in the case of the southeastern Australian passive margin, the relationship between the amount of escarpment retreat and offshore stratal patterns suggests that the offshore stratigraphic offlap is caused by onshore rift shoulder erosion. This can be explained by flexural rebound as a response to erosional unloading in the rift shoulder area. The rebound extends far into the basin and causes uplift of the shelf area and, as a consequence, a relative sea level fall. In the remainder of this paper we investigate, by using a numerical forward model, the effects on the resulting stratal patterns of a number of parameters influencing rift shoulder uplift, flexural isostasy, and erosion and redistribution of surficial sediments.

3. Lithospheric evolution model

A variety of models explaining uplift of rift flanks have been proposed. These models can be classified into transient and permanent uplift mechanisms. Transient models invoke a thermal mechanism to explain uplift (e.g., lateral heat transfer, small-scale asthenospheric convection, depth-dependent stretching). Permanent uplift, on the other hand, is explained by magmatic underplating, flow of lower crust, and the flexural response to lithospheric unloading and plastic necking [34–37]. Thermal mod-

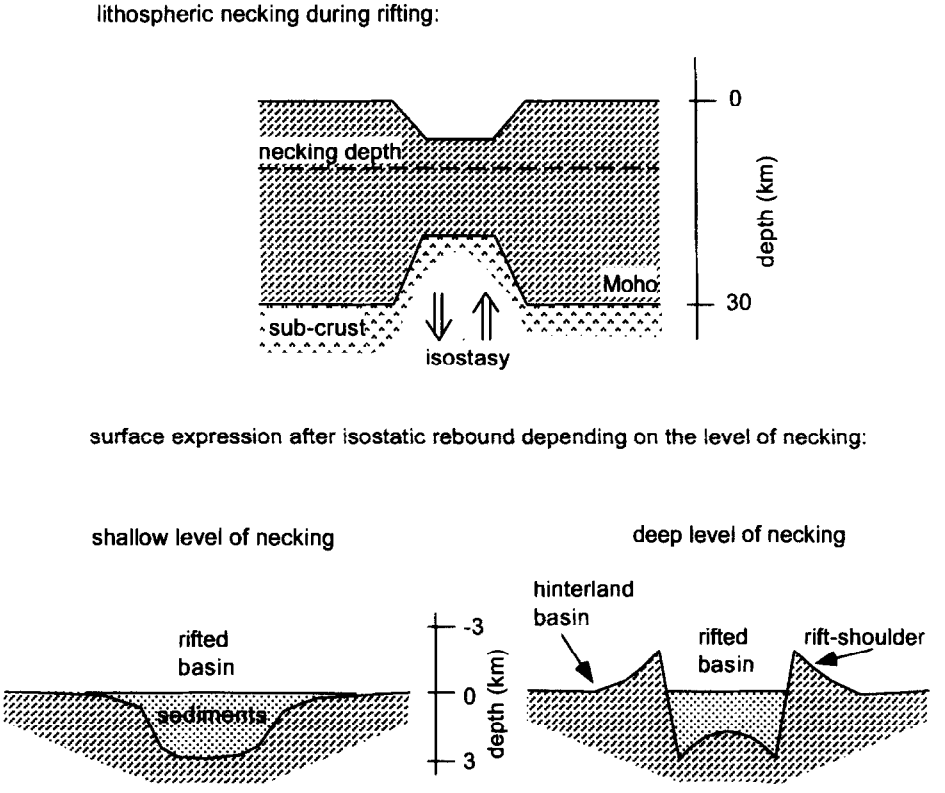

Fig. 5. The concept of lithospheric necking. The lithosphere is kinematically thinned around a level of necking. Depending on the amount of thinning and the level of necking, the basin may become overdeepened during the extension process. As a result, the basin and its margins are uplifted, leading to flexurally supported rift shoulders (after [39]).

els are not compatible with the inferred long lifespan of marginal uplifts [3,36,37] and the amount of observed or inferred uplift [7]. Magmatic underplating may be important in some cases (e.g., volcanic margins and flood basalt provinces), but does not generally occur along rifted margins. Because there are several lines of evidence indicating that the continental lithosphere may behave as a relatively strong elastic plate [15,38], permanent uplift can be explained by retention of flexural strength of the lithosphere during rifting, causing uplift in response to tectonic unloading or plastic necking [35–37]. This seems to be the mechanism which best explains the general occurrence of uplifted rift flanks [3,39].

We model the effect of rift shoulder erosion on offshore stratigraphic patterns by means of a two-dimensional model for lithospheric evolution. Our approach employs the pure-shear extension model of McKenzie [40], which uses extension factors defining kinematicaly the amount of lithospheric and crustal thinning at the passive margin. In the pure-shear model model, lithospheric cooling after thinning causes differential vertical motions to take place at the passive margin. We have extended the pure-shear model in order to take into account flexural compensation of lithospheric and sedimentary loads, two-dimensional heat flow, finite duration of rifting, and necking of the lithosphere during rifting around its strongest part(s) [39,41]. When a basin is overdeepened due to the necking process, the flexural isostatic response to necking causes uplift of the rift shoulder (Fig. 5).

Dynamic models of rifted basin formation show that, during extension, the lithosphere necks around its strongest layer(s), usually a mid-crustal level [42–44]. Estimates of lithospheric necking depths by forward modelling of rift shoulder uplift and erosion by Van der Beek et al. [3] have resulted in necking depths of 10 and 30 km for the Saudi Arabian and Transantarctic flank uplifts respectively. Tectonostratigraphic forward modelling of Neogene Mediterranean extensional basins yields necking depths ranging from 8 to 25 km [39,45–47].

The flexural isostatic response of the lithosphere to lithospheric and sedimentary loads is calculated from a two-dimensional thin elastic plate equation [48]. The flexure equation is solved by means of a finite-difference scheme. The effective elastic thickness, T_e, is taken to be equal to the depth of the 450°C isotherm, except for two models investigating the influence of T_e on offshore stratal patterns. The 450°C isotherm seems to be the optimal isotherm for defining oceanic as well as continental T_e [15,17,38]. Burov and Diament [38] show that a distinction can be made between mechanically uncoupled and coupled continental lithosphere, which is related to thermal age and rheological stratification. In the latter case, the mechanically strong layers of continental lithosphere, generally occurring in the upper crust and upper part of the subcrust, effectively act as one elastic plate. Mechanically coupled continental lithosphere is associated with thermal ages in excess of 800 m.y. and haves T_e's that are approximately coincident with the depth to the 600°C isotherm. Thermally young, mechanically uncoupled continental lithosphere is characterized by T_e's equal to the depth to isotherms that are in the range 300–450°C. Therefore, the 450°C isotherm best represents average conditions. The influence of T_e on the modelling results is investigated in separate models adopting the 300 and 600°C isotherms.

The inferred large amounts of erosion at continental margins can partly be explained by flexural rebound in response to erosional unloading at rift shoulders [2,20,49–51]. The isostatic uplift is amplified when the flexural bulge from offshore sediment loading comes into phase with erosionally driven isostatic uplift [52].

4. Numerical erosion–sedimentation model

Our surface process model employs the advective–diffusive model developed by Beaumont et al. [53] for onshore erosion and sedimentation and a modification of the diffusion model of Kaufman et al. [54] for offshore (submarine) sedimentation. The onshore advection–diffusion model incorporates short-range diffusive hillslope processes and long-range advective fluvial transport. A similar model was employed by Van der Beek et al. [32] for modelling the morphological evolution or rift shoulders and was found to reproduce adequately topographic and erosional patterns. A local equilibrium sediment carrying capacity of the long-range transport system is defined which is proportional to the

local power of the river or stream, taken as the product of discharge and slope of the stream:

$$q_e = -K q_{dis} \frac{dh}{dl}$$

where q_e = equilibrium carrying capacity, K = proportionality constant, q_{dis} = discharge flux, h = height and l = length (see Table 1).

The discharge of the stream is related to upstream precipitation by conservation of water volume. Sediment is deposited when the amount of sediment being carried by the system is greater than the equilibrium carrying capacity, erosion takes place when the amount of sediment being carried is less than this capacity. If the sediment transport is in steady state during a simulation timestep (non-varying fluxes), the amount of deposition or erosion will depend on a reaction rate constant, l_f, and the difference between equilibrium carrying capacity and the actual sediment flux [55]:

$$\frac{\partial h}{\partial t} = -\frac{1}{l_f}(q_e - q_s)$$

where q_s = sediment flux. When the sediment advection velocity is constant, l_f is a material property, the erosion–deposition length scale required for the disequilibrium to be reduced by a factor of $1/e$ when q_e is constant [55]. In our model, two types of transported material, basement rock and sediment, are distinguished. Furthermore, the amount of precipitation is constant across the modelling transect, which leads to a simple relationship between the discharge flux and the precipitation rate:

$$q_{dis} = q_{rain}|x - x_d|$$

where q_{rain} = precipitation rate and $|x - x_d|$ = distance to drainage divide.

The hillslope and offshore (submarine) sedimentation and erosion processes in our numerical model are based on a diffusion algorithm [56,57]. In this approach, sediment fluxes are proportional to the local slope:

$$q_s = -K\frac{dh}{dl}$$

The local rate of deposition or erosion depends on the local divergence of sediment fluxes:

$$\frac{\partial h}{\partial t} = -\nabla q_s$$

The hillslope diffusivity depends on climate because the soil creation rate depends on humidity and the erodibility of soil is controlled by vegetation. A high diffusivity of basement rocks or sediments therefore represents either a highly erodable substratum or a weathering process which produces a cohesionless regolith [55] sufficiently rapidly.

Following Kaufman et al. [54], our offshore sedimentation model employs an exponentially decreasing diffusivity of sediments with increasing water depth. This is in accordance with the observation that the wave energy available to mobilize sediment on a marine shelf decays exponentially with water depth [54].

4.1. Numerical implementation

The resulting equations are solved for every timestep using an explicit finite difference scheme.

Table 1
Notation

β_{max}	maximum extension
$l_{f\text{-}sed}$, $l_{f\text{-}bas}$	depositional length scales
$K_{diff\text{-}bas}$, $K_{diff\text{-}sed,\ areal}$, $K_{diff\text{-}sed,\ marine}$	areal transportation diffusivities; water-depth-defined marine trans. diff.
Kq_{rain}	rain fall times proportionality constant
H_{elev}	pre-rift continental elevation
Z_{neck}	depth of lithospheric necking
T_e	effective elastic thickness
T_{flex}	isotherm defining the effective elastic thickness
wd	water depth

The first step consists of locating the drainage divides in the cross section. Then, starting from a divide, downslope sediment fluxes are tracked. When a grid node is located above sea level advection of sediment is calculated: precipitation is integrated upstream and used to calculate the local deposition or erosion. For the same timestep, sediment transport due to hillslope diffusion is calculated. When a grid node is below sea level only diffusion is applied, with a diffusivity defined by the water depth.

A general outline of the two-dimensional model is shown in Fig. 6. With the exception of models used to investigate the influence of this assumption, the models conserve the mass of bedrock and sediments in two dimensions (i.e., all the erosion products of the rift shoulder are ultimately deposited as sediments in the basin). Erosion products on the landward side of the rift shoulder are first deposited in the flexural hinterland basin. Eventually, due to overfilling of this basin or its uplift and erosion due to the landward migrating rift shoulder escarpment, these sediments leave the model at the boundary (fixed height numerical boundary condition) and are reintroduced at the shoreline position. This simulates the redistribution of hinterland basin sediments by major river systems breaching the marginal upwarp and draining the hinterland basin (e.g., the southern African Orange River). These river systems transport large amounts of clastics from the hinterland basin to the upper shelf area, where they are redistributed by longshore currents. Thus, essentially mass is conserved in a section perpendicular to the rift shoulder. Erosional products from the basinward side of the rift shoulder are directly transported into the offshore part of the extensional basin.

The erosion–sedimentation model is linked to the subsidence model in two different ways. Firstly, the erosion and redistribution of surficial mass changes the loads acting on the elastic plate used to calculate flexural isostasy. Removal of sediment or bedrock results in isostatic uplift, sediment deposition causes subsidence. Secondly, through coupling with the temperature model the erosion of bedrock causes a loss of heat energy and, as a result, an increase in the thermal gradient occurring in the surficial part of the crust. As a consequence, the depth to the isotherm used to define T_e reduces due to the erosion.

5. Modelling of the effects of rift shoulder erosion on stratigraphy

In this section we explore the influence of a number of key parameters controlling the style and amount of uplift and erosion of rift shoulders and resulting basin fill by analyzing different models of

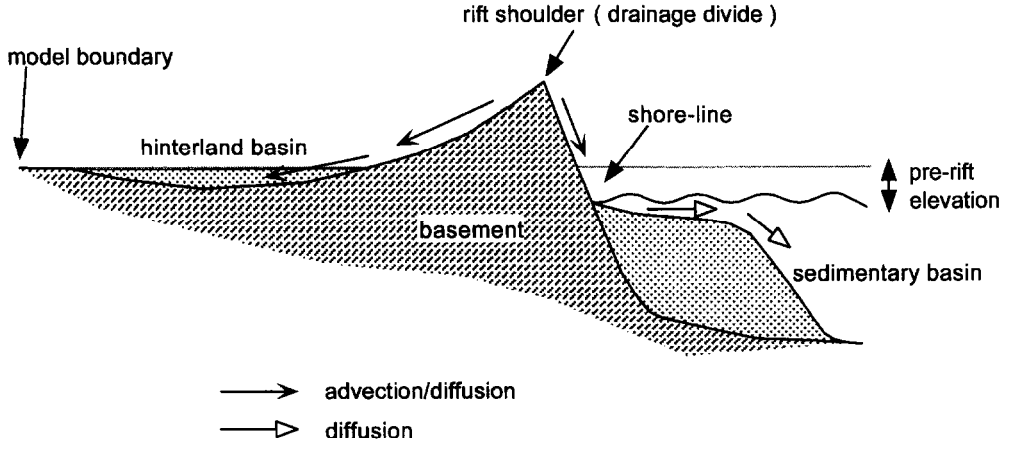

Fig. 6. Cartoon of the rift shoulder erosion model. The isostatic response to necking of the lithosphere during extension causes a flexuraly supported rift shoulder. In a landward direction the rift shoulder is flanked by a flexural downwarp, the hinterland basin. The erosion products of the rift shoulder are transported to the offshore rifted basin and the hinterland basin. When the hinterland basin is completely filled, the sediments are taken out at the location indicated by 'model boundary'. These sediments are reintroduced into the model at the shoreline position in the offshore basin, establishing conservation of mass in the model.

Table 2
Parameters for all models

β_{max}	3.0
$l_{f\text{-}sed}$	50 km
$l_{f\text{-}bas}$	5 km
$K_{diff\text{-}bas}$	1 m^2/yr
$K_{diff\text{-}sed,\ areal}$	5 m^2/yr
$K_{diff\text{-}sed,\ marine}$	$5 \cdot 10^3 \cdot \exp(-wd)$ m^2/yr

basin evolution and by varying the depth of lithospheric necking, the erosion rate of the rift shoulder, the pre-rift continental elevation and other, less important, parameters. We define a reference model for the evolution of a margin subjected to erosion of a flexurally supported rift shoulder. The influences of the parameters mentioned above are illustrated by comparing differences with the reference model. We will begin with an outline of the modelling parameters and results for the reference model.

Values for parameters controlling the on-and offshore erosion and deposition have been taken from Kooi and Beaumont [55] and Kaufman et al. [54] respectively. The applied values for the parameters concerning the flexural reference model (FRM) are given in Tables 2 and 3 (for notation, see Table 1). In the flexural models the extension factors increase linearly from the hinge zone to a value of β_{max} (3.0) at a distance of 50 km in the basinward direction, reflecting the gradual basinward increase in the amount of extension commonly observed at passive margins. The rifting duration is taken to be instantaneous, unless otherwise stated.

The modelling results depicted in the upper panel of Fig. 7 show the evolution of the rift shoulder, hinterland basin and offshore stratigraphy for the first 150 m.y. after rifting. The ages of the different rift shoulder profiles and stratigraphic layers are indicated in the figure. Generally, the result shows a steadily retreating rift shoulder and hinterland basin system. The tectonically uplifted rift shoulder is completely eroded within 50 m.y. The remnant escarpment results from isostatic rebound and retreats landward with a velocity of 1 m/m.y. The total amount of predicted erosion at the former rift shoulder after 150 m.y. is about 3.5 km. The exhumation histories for three different locations are depicted in Fig. 8. These results are largely in agreement with forward modelling of rift shoulder erosion by Van der Beek et al. [32]. The offshore stratigraphy displays a prograding sedimentary wedge. It is noteworthy that the large-scale stratigraphy does not show major onlap onto the basin margin: only about 16 km of stratigraphic onlap is observed after an initial offlap of ~ 15 km during the first 15 m.y. of basin evolution. This is mainly due to the relief created by the rift shoulder and the long time span required to erode it. The latter variable is important because the onlap-promoting mechanisms are to a great extent thermally controlled (increase in flexural rigidity and increase in lithospheric contraction loads). The thermal time constant has a value of about 50 m.y., indicating that the onlap-promoting mechanisms have largely decayed by the time the rift shoulder is eroded. Therefore, only a small amount of onlap is produced in this model. The lower panel of Fig. 7 shows a close-up of the stratal patterns after 50 m.y. This figure clearly demonstrates that during the first 15 m.y. of post-rift basin evolution the sedimentary wedge is strongly offlapping; the position of landward lapout migrates about 15 km basinward. The mechanism responsible for this offlapping pattern is isostatic rebound due to erosion of the rift shoulder, causing flexural uplift extending far into the basin. A cartoon of this mechanism is depicted in Fig. 9. The total predicted amount of flexural uplift in the shelf

Table 3
Other parameter values and model differences

	Ref. model	Faster erosion	Slower erosion	Higher elevation	Lower elevation	Higher isotherm	Lower isotherm	Deeper neck
Z_{neck}	15 km							25
Kq_{rain}	0.01 m/yr	0.02	0.005					
H_{elev}	500 m			1000	100			
T_{flex}	450°C					600	300	

area after 15 m.y. is about 500 m, indicating an average uplift rate of 33 m/m.y.

In order to understand the influence of the different parameters on the resulting stratigraphic patterns and erosion rates, we have performed a sensitivity analysis. For each case presented we change the value of only one parameter and compare the results to the reference model.

In Fig. 10 we depict the position of landward lapout as a function of time (i.e., coastal onlap curves) for the different models investigated. Firstly, we compare the results of the flexural reference model (FRM) to thermal models for marginal uplift. Using a model in which lateral heatflow causes a slight marginal uplift, Watts et al. [15] analyzed the pattern of coastal onlap at passive margins. However, their model did not consider erosion of the (small) uplift. The thermal model we have constructed produces a marginal uplift by extending the subcrustal lithosphere over a larger area than the crust [16], causing a thermally induced 1.3 km high uplift at the basin edge. The resulting uplift is eroded by the same mechanisms as in the FRM. A comparison between the prediction of coastal onlap by the thermal model of Watts et al. [15], the FRM and the thermal model we have developed is shown in Fig. 10a. The two thermal models show the same general pattern consisting of fast, continuous stratigraphic onlap. The initial offlapping observed in the FRM is not observed in the thermal models, indicating that the onlap-promoting mechanisms (related to lithospheric cooling) were more important, despite the erosionally induced flexural rebound in our thermal model. The difference in the total amount of coastal

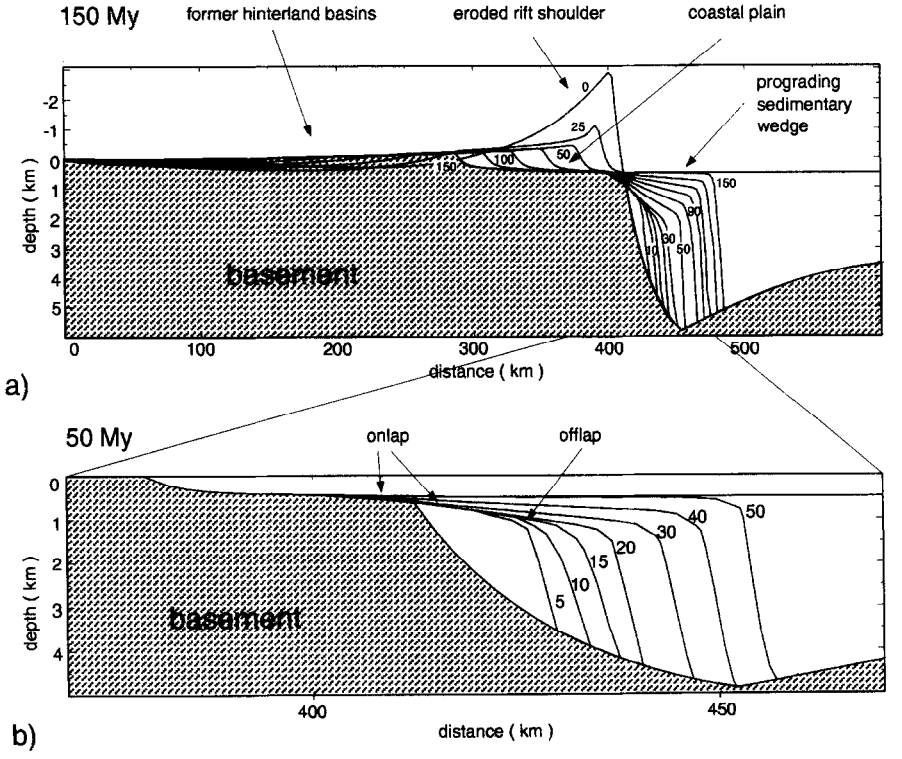

Fig. 7. (a) Overview of the flexural reference model (FRM) after 150 m.y. The left-hand part of the figure shows the evolution of the hinterland basin and the retreat of the rift shoulder. The right-hand part displays the resulting stratigraphy in the offshore extensional basin (passive margin). The numbers indicate ages (m.y.) of morphological and depositional surfaces. (b) Close-up of the stratigraphy in the extensional basin after 50 m.y. of margin evolution. The stratigraphy clearly demonstrates the offlapping nature of the first post-rift sediments. At 15 m.y. a total offlap of 15 km is observed in the modelling result. The offlap is caused by 500 m of flexural uplift in response to rift shoulder erosion.

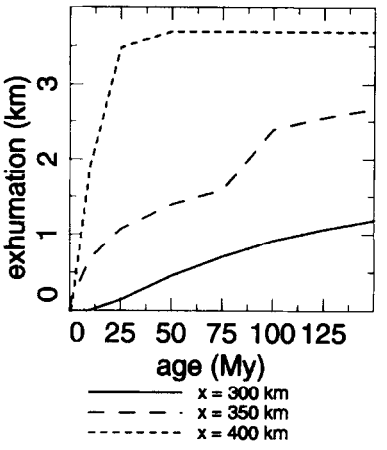

Fig. 8. Exhumation histories for three locations at distances of 300, 350 and 400 km along the cross section of Fig. 7. The relatively slow exhumation at the location at a distance of 300 km along the cross section is entirely controlled by the low gradients occurring at the landward site of the rift shoulder uplift. The initial fast exhumation at the location at a distance of 400 km is caused by the locallly high topographic gradients at the escarpment. The acceleration of exhumation starting at 80 m.y. for the location at a distance of 350 km reflects the passage of the escarpment during its retreat.

onlap between the FRM and the thermal models is very large (about 50 km after 50 m.y.).

By varying the amount of precipitation in the model (i.e., Kq_{rain}) we compare cases with different erosion efficiencies (Table 3). The effect of erosion rate on the evolution of offshore stratigraphic patterns is shown in Fig. 10b. Faster erosion (Kq_{rain} increased by a factor of 2) causes about the same offlap (15 km), but due to the more rapid scarp retreat the duration of offlapping is shorter (7.5 m.y. instead of 15). Slower erosion produces much less offlap (5 km in total) and also a shorter duration of offlapping; the onlap-promoting mechanisms overcome the erosional rebound rate after less time. The overall stratigraphy for the 'slower' model displays a less evolved coastal onlap pattern compared to the FRM, lagging continuously behind the FRM.

The next set of models (Fig. 10c) was designed to shed light on the influence of pre-rift continental elevation. Pre-rift continental elevation also exerts a primary control on the onshore morphology of the margin (see Van der Beek et al. [32]). The greater the difference between sea level and continental elevation, the greater the amount of bedrock to be eroded. This results in more erosional rebound and more offshore sedimentary loading. However, because more rock mass must be eroded, the retreat of the escarpment will also be slower. The modelling results indicate that a higher pre-rift elevation causes more offlap (17.5 km), but, mainly due to slower escarpment retreat, the coastal onlap does not proceed as far as in the FRM. The model with a lower

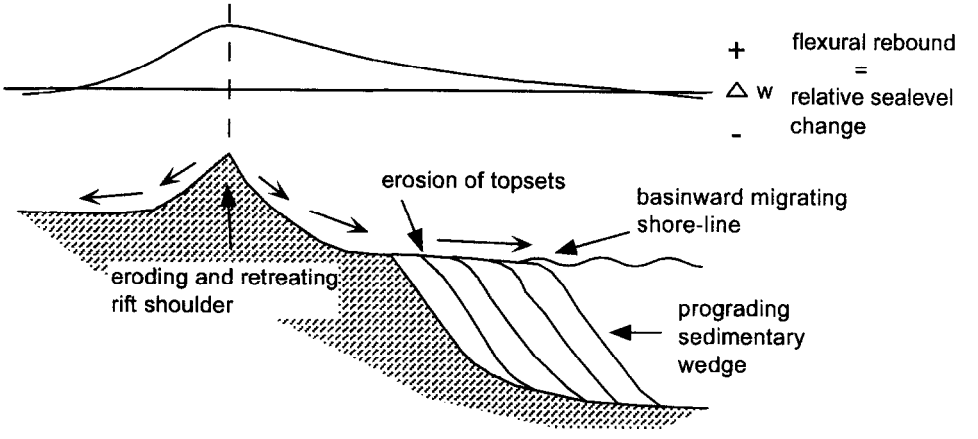

Fig. 9. Cartoon illustrating the mechanism of initial post-rift coastal offlap at passive margins. Flexural rebound in response to erosional unloading at the rift shoulder causes uplift extending far into the offshore basin. The uplift causes erosional truncation of the topsets of the sedimentary wedge. Coastal onlap will occur when the rate of erosion-induced uplift is less than the subsidence caused by sedimentary loading, thermal contraction and the flexural response to the increase in rigidity. Δw = instantaneous flexural uplift (+) and subsidence (−) pattern caused by rift shoulder erosion.

initial continental elevation produces much less offlap and a more rapidly progressing coastal onlap, as a result of less erosional rebound.

We have also investigated the effect of two parameters influencing flexural isostasy, the isotherm which defines the effective elastic thickness of the lithosphere and the depth of necking of the lithosphere during rifting (Table 3). The results are shown in Fig. 10d. The effect of using a lower isotherm defining the effective elastic thickness (300°C) on the stratigraphic patterns is very small. The same amount and duration of offlapping are produced, only the total amount of onlap is slightly less than in the FRM. The results of a model adopting a higher isotherm (600°C) show less initial offlap and, eventually, also less onlap. This is caused by the decreasing amplitude and increasing wavelength of the flexural isostasy with increasing T_e. The influence of the depth of necking is more dramatic. A deeper level of necking not only produces more flexural uplift but also considerably alters the flexural state of the lithosphere underlying the remainder of the basin [39]. The resulting stratigraphy in this model displays more offlap (20 km), which also lasts longer than in

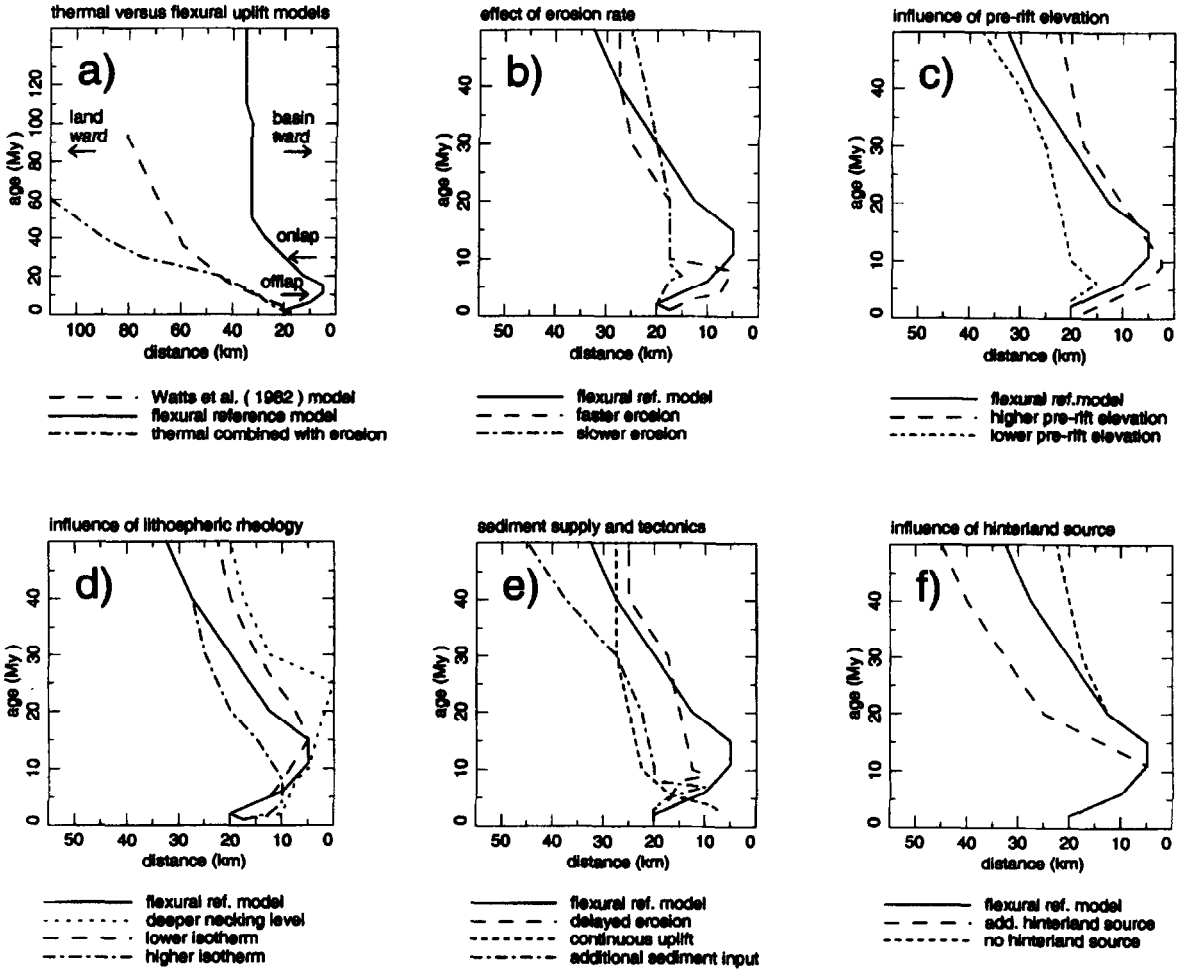

Fig. 10. (a) The resulting coastal onlap patterns for two thermal uplift models and the flexural reference model. The main differences between the flexural reference model and the thermal models are the lesser extent of coastal onlap and the occurrence of an initial offlap pattern in the first post-rift stratigraphy. (b–f) The results of the other flexural models, constructed to examine the effects of variations in T_e, necking depth, erosion rates and timing of erosion, confirm the pattern predicted by the FRM. See text for further discussion.

the FRM (25 m.y.). Because it takes longer to erode the (higher) rift shoulder in this model, the thermally controlled onlap-promoting mechanisms are less successful in generating flank subsidence. The resulting large-scale stratigraphic onlap does not proceed as far as in the FRM. This model produces a maximum amount of erosion of about 6 km at the location of the summit of the initial rift shoulder. The total amount of flexural uplift at the shelf is 780 m, indicating an average uplift rate of about 30 m/m.y.

The results of more exotic models are displayed in Fig. 10e. A model delaying the initiation of rift shoulder erosion by 50 m.y. displays less initial offlap and a smaller total amount of onlap after 150 m.y., compared to the FRM. This can be explained in terms of cooling-induced strengthening of the lithosphere, as a result of which less initial erosional rebound (offlap) and less general flexural downbending (onlap) is produced. Delayed erosion of the rift shoulder could be the consequence of climatic conditions. A model invoking continuous extension for 150 m.y. does not produce a rift shoulder because erosion rates keep up with tectonic uplift. Therefore, the stratigraphy of this model displays thermally controlled continuous onlap. A model adopting an additional external sediment source shows that the loading effect of the additional sediments strongly diminishes the initial offlap and promotes large-scale onlap. Such a situation could occur in large delta systems.

Finally, Fig. 10f shows the influence of the assumption concerning the conservation of mass in the modelled cross section. In the previous models, sediments leaving the model at the landward side of the hinterland basin are reintroduced in the cross section at the shoreline position, simulating the drainage of the hinterland basin by major river systems breaching the rift flank uplift. In this set of models we have modelled two alternative cases. In one model, 5 times the amount of sediment that leaves the model at the border of the hinterland basin is (re-) introduced at the shoreline position. This could reflect the situation at the location where a river system breaches a marginal upwarp. In the other model, no sediments are reintroduced at the shoreline position, simulating the circumstances far from breaching rivers. The results show that the mass-conservation assumptions do not influence the amount of inital offlap, because during this time period the hinterland basin does not yet contain sufficient sediment to become overfilled. However, during the later stage of basin evolution the model with additional hinterland basin sediment input produces more onlap than the FRM, which can be explained by enhanced flexural downbending of the basin flank as a response to a larger sediment load. The model adopting zero hinterland sediment input produces less onlap as a result of less sediment loading.

6. Discussion and conclusions

Our models demonstrate that erosion of flexurally supported rift shoulders produces a different stratal onlap pattern compared to models invoking thermal mechanisms to explain marginal uplift. A typical flexurally induced stratal pattern is characterized by initial offlap. The offlap is succeeded by onlap, which extends, however, far less landward than for thermal models. Together, the initial offlap and succeeding onlapping wedges form one complete second-order sequence (as defined by Vail et al. [12], second-order sequences last 10–80 m.y.). The amount and duration of initial offlap are enhanced by deeper necking depths during rifting and higher continental pre-rift elevations. The average flexural uplift rate at the shelf produced by our models is about 30 m/m.y.

In our model for passive margin evolution, large-scale onlap onto the coastal plain area (initially occupied by the rift shoulder), as observed on the southeastern Brazilian and U.S. east coast margins, can only be explained by a large regional relative sea level rise. In fact, because in a late stage of the modelled temporal evolution the coastal area is always eroded to sea level, any major eustatic sea level rise would cause an immediate flooding of the coastal plain area. Therefore, the first sediments covering the entire coastal plain must be the result of a large regional sea level highstand. However, the timing of highstands for these margins is completely different —Eocene for the southeastern Brazilian margin compared to Early Cretaceous for the U.S. east coast margin. There seems to be no clear-cut evidence for a large Eocene highstand on the U.S. margin and, as discussed before, the Early Cretaceous strata of the

Brazilian margin display evidence for a regional relative sea level fall. An explanation for this discrepancy could be the differences in physiography, subsidence rate and sediment supply, causing different responses to eustatic sea level changes [58–60]. Alternatively, the inferred large relative sea level rises can be caused by regional tectonic processes. For example, varying intraplate stress levels can lead to the development of short-term on-and offlap patterns, generating second-and third-order stratigraphic sequences [61,62].

Coastal onlap is traditionally interpreted as a general feature of passive margin stratigraphy by basin evolution models [15] and sequence stratigraphy [12,63]. It is considered to be a continuous feature, punctuated by tectonics and eustatic sea level changes. However, inspection of the early post-rift stratigraphy at passive margins with abundant evidence for (formerly) uplifted rift flanks (i.e., the U.S. east coast, the southeastern Brazilian and southeastern Australian margins and the Transantarctic Mountains–Ross Sea Shelf system) shows that they comprise largely offlapping stratigraphic signatures. Our modelling of rift flank erosion and offshore deposition demonstrates that the initial offlap can be explained as the result of flexural uplift of the shelf area in response to erosional unloading of the uplifted rift flanks. These findings have profound implications for the interpretation of coastal onlap patterns in terms of eustatic or tectonic causes. In the deriviation of the global eustatic chart, Haq et al. [64] assumed that passive margins show a continuous smooth and slow relative sea level rise due to thermal and sediment loading processes. In contrast, our modelling results and data from a number of rifted passive margins indicate that the first part of the post-rift phase will be in general characterized by a relative sea level fall and stratigraphic offlap.

Acknowledgements

We thank three anonymous reviewers for useful comments and suggestions. We also thank Henk Kooi for introducing us to the advective–diffusive surface process model. This research was carried out in the framework of the IBS (Integrated Basin Studies) Project, which is part of the JOULE II research programme funded by the Commission of European Communities (contract JOU2-CT 92-0110). This is IBS contribution 10 and publication 950404 of the Netherlands Research School for Sedimentary Geology. [*UC*]

References

[1] C.J. Ebinger, A.L. Deino, A.L. Tesha, T. Becker and U. Ring, Tectonic controls on rift basin morphology: evolution of the northern Malawi (Nyasa) rift, J. Geophys. Res. 98, 17821–17836, 1993.

[2] M.S. Steckler and G.I. Omar, Controls on erosional retreat of the uplifted rift flanks at the Gulf of Suez and northern Red Sea, J. Geophys. Res. 99, 12159–12173, 1994.

[3] P. van der Beek, S. Cloetingh and P. Andriessen, Mechanisms of extensional basin formation and vertical motions at rift flanks: Constraints from tectonic modelling and fission track thermochronology, Earth Planet. Sci. Lett. 121, 417–433, 1994.

[4] D.J. Rust and M.A. Summerfield, Isopach and borehole data as indicators of rifted margin evolution in southwestern Africa, Mar. Pet. Geol. 7, 277–287, 1990.

[5] R.W. Brown, D.J. Rust, M.A. Summerfield, A.J.W. Gleadow and M.C.J. de Wit, An Early Cretaceous phase of accelerated erosion on the south-western margin of Africa: evidence from apatite fission track analysis and the offshore sedimentary record, Nucl. Tracks Radiat. Meas. 17, 339–350, 1990.

[6] U. ten Brink and T. Stern, Rift flank uplifts and hinterland basins: comparison of the Transantarctic Mountains with the Great Escarpment of southern Africa, J. Geophys. Res. 97, 569–585, 1992.

[7] K. Gallagher, C.J. Hawkesworth and M.S.M. Mantovani, The denudation history of the onshore continental margin of SE Brazil inferred from apatite fission track data, J. Geophys. Res. 99, 18117–18145, 1994.

[8] D.S. Miller and I.R. Duddy, Early Cretaceous uplift and erosion of the northern Appalachian Basin, New York, based on apatite fission track analysis, Earth Planet. Sci. Lett. 93, 35–49, 1989.

[9] M.S. Steckler, G.I. Omar, G.D. Karner and B.P. Kohn, Pattern of hydrothermal circultation within the Newark basin from fission-track analysis, Geology 21, 735–738, 1994.

[10] M.E. Moore, A.J.W. Gleadow and J.F. Lovering, Thermal evolution of rifted continental margins: new evidence from fission tracks in basement apatites from southeastern Australia, Earth Planet. Sci. Lett. 78, 255–270, 1986.

[11] T.A. Dumitru, K.C. Hill, D.A. Coyle, I.R. Duddy, D.A. Foster, A.J.W. Gleadow, P.F. Green, B.P. Kohn, G.M. Laslett and A.J. O'Sullivan, Fission track thermochronology: application to continental rifting of south-eastern Australia, APEA J., pp. 131–142, 1991.

[12] P.R. Vail, R.M. Mitchum, Jr., R.G. Todd, J.M. Widmier, S. Thompson, III, J.B. Sangree, J.N. Bubb and W.G. Hatlelid,

Seismic stratigraphy and global changes of sea level, in: Seismic Stratigraphy—Applications to Hydrocarbon Exploration, C.E. Payton, ed., Am. Assoc. Pet. Geol. Mem. 26, 49–212., 1977.

[13] S. Cloetingh, A.J. Tankard, H.J. Welsink and W.A.M. Jenkins, Vail's coastal onlap charts and their correlation with tectonic events, offshore eastern Canada, in: Extensional Tectonics and Stratigraphy of the North Atlantic Margin, A.J. Tankard and H.R. Balkwill, eds., Am. Assoc. Petrol. Geol. Mem. 46, 283–293, 1989.

[14] W.E. Galloway, Genetic stratigraphic sequences in basin analyses II: application to the northwest Gulf of Mexico Cenozoic Basin, Am. Assoc. Pet. Geol. Bull. 73, 143–154, 1989.

[15] A.B. Watts, G.D. Karner and M. Steckler, Lithospheric flexure and the evolution of sedimentary basins, Philos. Trans. R. Soc. London 305, 249–281, 1982.

[16] N. White and D. McKenzie, Formation of the 'steer's head' geometry of sedimentary basins by differential stretching of the crust and mantle, Geology 16, 250–253, 1988.

[17] C. Beaumont, C.E. Keen and R. Boutilier, On the evolution of rifted continental margins: comparison of models and observations for the Nova Scotia margin, Geophys. J. R. Astron. Soc. 70, 667–715, 1982.

[18] A.B. Watts, Lithospheric flexure due to prograding sediment loads: implications for the origin of offlap/onlap patterns in sedimentary basins, Basin Res. 2, 133–144, 1989.

[19] R.J. Hubbard, Age and significance of sequence boundaries on Jurassic and Early Cretaceous rifted continental margins, Am. Assoc. Pet. Geol. Bull. 72, 49–72, 1988.

[20] A.R. Gilchrist, H. Kooi and C. Beaumont, Post-Gondwana geomorphic evolution of southwestern Africa: implications of the controls on landscape development from observations and numerical experiments, J. Geophys. Res. 99, 12211–12228, 1994.

[21] J.A. Grow, K.D. Klitgord and J.S. Schlee, Structure and evolution of the Baltimore Canyon Trough, in: The Atlantic Continental Margin, U.S. (The Geology of North America, Vol. I-2), R.E. Sheridan and J.A. Grow, eds., pp. 269–290, Geol. Soc. Am., Boulder, Colo., 1988.

[22] F.J. Pazzaglia and T.W. Gardner, Late Cenozoic flexural deformation of the middle U.S. Atlantic passive margin, J. Geophys. Res. 99, 12143–12157, 1994.

[23] D.T. Lawrence, M. Doyle and T. Aigner, Stratigraphic simulation of sedimentary basins: concepts and calibration, Am. Assoc. Pet. Geol. Bull. 74, 273–295, 1990.

[24] S.M. Greenlee and T.C. Moore, Recognition and interpretation of depositional sequences and calculation of sea-level changes from stratigraphic data—offshore New Jersey and Alabama Tertiary, in: Sea-Level Changes—an Integrated Approach, C.K. Wilgus, B.S. Hastings, C.G.St.C. Kendall, H.W. Posamentier, C.A. Ross and J.C. van Wagoner, eds., Soc. Econ. Paleontol. Mineral. Spec. Publ. 42, 29–353, 1988.

[25] W.U. Mohriak, G.D. Karner, J.F. Dewey and J.R. Maxwell, Structural and stratigraphic evolution of the Campos Basin, offshore Brazil, in: Extensional Tectonics and Stratigraphy of the North Atlantic Margin, A.J. Tankard and H.R. Balkwill, eds., Am. Assoc. Pet. Geol. Mem. 46, 577–598, 1988.

[26] P.G. Fitzgerald, The Transantarctic Mountains of southern Victoria Land: the application of fission track analysis to a rift shoulder uplift, Tectonics 11, 634–662, 1992.

[27] A.K. Cooper, F.J. Davey and K. Hinz, Crustal extension and origin of sedimentary basins beneath the Ross Sea and Ross Ice Shelf, Antarctica, in: Geological Evolution of Antarctica, M.R.A. Thomson, J.A. Crame and J.W. Thomson, eds., pp. 285–291, Cambridge University Press, Cambridge, 1991.

[28] A.K. Cooper, F.J. Davey and J.C. Behrendt, Structural and depositional controls on Cenozoic and (?)Mesozoic strata beneath the western Ross Sea, in: Geological Evolution of Antarctica, M.R.A. Thomson, J.A. Crame and J.W. Thomson, eds., pp. 279–283, Cambridge University Press, Cambridge, 1991.

[29] L.R. Bartek, P.R. Vail, J.B. Anderson, P.A. Emmet and S. Wu, Effect of Cenozoic ice sheet fluctuations in Antarctica on the stratigraphic signature of the Neogene, J. Geophys. Res., 96, 6753–6778, 1991.

[30] B.P. Davies, Shallow seismic structure of the continental shelf, southeast Australia, J. Geol. Soc. Aust. 22, 345–359, 1975.

[31] C.D. Ollier and C.F. Plain, Landscape evolution and tectonics in southeastern Australia, AGSO J. Aust. Geol. Geophys. 15, 335–345, 1994.

[32] P. van der Beek, P. Andriessen and S. Cloetingh, Morphotectonic evolution of rifted continental margins; inferences from a coupled tectonic–surface processes model and fission-track thermochronology, Tectonics 14, 406–421, 1995.

[33] C.D. Ollier, The Great Escarpment of eastern Australia: tectonic and geomorphic significance, J. Geol. Soc. Aust. 29, 13–23, 1982.

[34] M.H.P. Bott, Formation of sedimentary basins of graben type by extension of continental crust, Tectonophysics 36, 77–86, 1976.

[35] J. Braun and C. Beaumont, A physical explanation of the relationship between flank uplifts and the breakup unconformity at rifted continental margins, Geology 17, 760–764, 1989.

[36] J.K. Weissel and G.D. Karner, Flexural uplift of rift flanks due to mechanical unloading of the lithosphere during extension, J. Geophys. Res. 94, 13919–13950, 1989.

[37] J. Chéry, F. Lucazeau, M. Daignières and J.P. Vilotte, Large uplift at rift flanks: a genetic link with lithospheric rigidity? Earth Planet. Sci. Lett. 112, 195–211, 1992.

[38] E.B. Burov and M. Diament, The effective elastic thickness (T_e) of continental lithosphere: what does it really mean? J. Geophys. Res. 100, 948–956, 1995.

[39] H. Kooi, S. Cloetingh and J. Burrus, Lithospheric necking and regional isostasy at extensional basins 1. Subsidence and gravity modelling with an application to the Gulf of Lions margin (SE France), J. Geophys. Res. 97, 17553–17571, 1992.

[40] D.P. McKenzie, Some remarks on the development of sedimentary basins, Earth Planet. Sci. Lett. 40, 25–31, 1978.

[41] R.T. van Balen and S. Cloetingh, Tectonic control of the

sedimentary record and stress-induced fluid flow: constraints from basin modelling, in: Geofluids: Origin, Migration and Evolution of Fluids in Sedimentary Basins, J. Parnell, ed., Geol. Soc. London Spec. Publ. 78, 9–26, 1994.

[42] M. Zuber and E.M. Parmentier, Lithospheric necking: a dynamic model for rift morphology, Earth Planet. Sci. Lett. 77, 373–383, 1986.

[43] J. Braun and C. Beaumont, Contrasting styles of lithoshperic extension: implications for differences between the Basin and Range province and rifted continental margins, in: Extensional Tectonics and Stratigraphy of the North Atlantic Margins, A.J. Tankard and H.R. Balkwill, eds., Am. Assoc. Pet. Geol. Mem. 46, 53–80, 1989.

[44] G. Bassi, C.E. Keen and P. Potter, Contrasting styles of rifting: models and examples from the eastern Canadian margin, Tectonics 12, 639–655, 1993.

[45] M.E. Janssen, M. Torné, S. Cloetingh and E. Banda, Pliocene uplift of the eastern Iberian margin: inferences from quantitative modelling of the Valencia Trough, Earth Planet. Sci. Lett. 119, 585–598, 1993.

[46] R.T. van Balen, L. Lenkey, F. Horváth and S. Cloetingh, Numerical modelling of stratigraphy and fluid flow in the Pannonian Basin, Am. Assoc. Pet. Geol., submitted.

[47] G. Spadini, S. Cloetingh and G. Bertotti, Thermo-mechanical modelling of the Tyrrhenian Sea: lithospheric necking and kinematics of rifting, Tectonics 14, 629–644, 1995.

[48] D.L. Turcotte and G. Schubert, Geodynamics, Application of Continuum Physics to Geological Problems, 450 pp., Wiley, New York, 1982.

[49] R. Stephenson and K. Lambeck, Erosion-isostatic rebound models for uplift: an application to south-eastern Australia, Geophys. J. R. Astron. Soc. 82, 31–55, 1985.

[50] Z. Garfunkel, Relation between continental rifting and uplifting: evidence from the Suez rift and northern Read Sea, Tectonophysics 150, 33–49, 1988.

[51] A.R. Gilchrist and M.A. Summerfield, Differential denudation and flexural isostasy in formation of rifted-margin upwarps, Nature 346, 739–742, 1990.

[52] G.E. Tucker and R.L. Slingerland, Erosional dynamics, flexural isostasy, and long-lived escarpments: a numerical modeling study, J. Geophys. Res. 99, 12229–12243, 1994.

[53] C. Beaumont, P. Fullsack and J. Hamilton, Erosional control of active compressional orogens, in: Thrust Tectonics, K.R. McClay, ed., pp. 1–18, Chapman and Hall, London, 1992.

[54] P. Kaufman, J.P. Grotzinger and D.S. McCormick, Depth-dependent diffusion algorithm for simulation of sedimentation in shallow marine depositional systems, in: Sedimentary Modeling: Computer Simulations and Methods for Improved Parameter Definition, E.K. Franseen, W.L. Watney, C.G.St.C. Kendall and W. Ross, eds., pp. 489–508, Kans. Geol. Surv., Lawrence, Kansas, 1992.

[55] H. Kooi and C. Beaumont, Escarpment evolution on high-elevation rifted margins: Insights derived from a surface process model that combines diffusion, advection, and reaction, J. Geophys. Res. 99, 12191–12209, 1994.

[56] W.E.H. Culling, Theory of erosion of soil-covered slopes, J. Geol. 73, 230–254, 1965.

[57] P.M. Kenyon and D.L. Turcotte, Morphology of a delta prograding by bulk sediment transport, Geol. Soc. Am. Bull. 96, 1457–1465, 1985.

[58] C.L. Angevine, Relationship of eustatic oscillations to regressions and transgressions on passive continental margins, in: Origin and Evolution of Sedimentary Basins and their Energy and Mineral Resources, R.A. Price, ed., Am. Geoph. Union Geophys. Monogr. 48, 29–35, 1989.

[59] H.W. Posamentier and G.P. Allen, Variability of the sequence stratigraphic model: effects of local basin factors, Sediment. Geol. 86, 91–109, 1993.

[60] W. Schlager, Accomodation and supply—a dual control on stratigraphic sequences, Sediment. Geol. 86, 111–136, 1993.

[61] S. Cloetingh, Tectonics and sealevel changes, a controversy? in: Controversies in Modern Geology: a Survey of Recent Developments in Sedimentation and Tectonics, D. Müller, H. Weissel and D. McKenzie, eds., pp. 249–277, Academic Press, London, 1991.

[62] R.T. van Balen and S. Cloetingh, The effects of intraplate stresses on sequence stratigraphy, Geology, submitted.

[63] C.K. Wilgus, B.S. Hastings, C.G.St.C. Kendall, H.W. Posamentier, C.A. Ross and J.C. van Wagoner, Sea-level changes —an integrated approach, Soc. Econ. Paleontol. Mineral. Spec. Publ. 42, 407, 1988.

[64] B. Haq, J. Hardenbol and P.R. Vail, Chronology of fluctuating sea levels since the Triassic, Science 235, 1156–1167, 1987.